Probabilistic amplitude shaping for a 64-QAM OFDM W-band RoF system

Probabilistic Amplitude Shaping for a 64-QAM OFDM W-band RoF System

Kaiquan Wu, Jing He, Zhihua Zhou, and Jin Shi

***Abstract*—In the paper, probabilistic amplitude shaping (PAS) is performed in the case of orthogonal frequency division multiplexing (OFDM) by combining with orthogonal circulant matrix transform (OCT) precoding. Thanks to the precoding method, one optimized probabilistic distribution is globally implemented across 240 subcarriers by merely one distribution matcher (DM). The proposed probabilistic shaping scheme for OFDM is experimentally demonstrated in a 64-ary quadrature amplitude modulation (QAM) W-band radio-over-fiber (RoF) system using direct-detection (DD), with 20-km single-mode fiber (SMF) and 0.5-m free-space transmission. Experimental results show that compared to the uniform 64-QAM, there is 1.07 dB shaping gain for system sensitivity at BER of 10^{-4}. Meanwhile, it inherits the advantage of flexible capacity granularity from the conventional single-carrier PAS.**

***Index Terms*—probabilistic amplitude shaping, OFDM, QAM, millimeter wave, radio over fiber communication.**

I. Introduction

The W-band (75~110 GHz) microwave signal exhibits advantages of precise directionality and low atmospheric attenuation, while radio-over-fiber (RoF) systems possess abundant bandwidth, low transmission loss, and high mobility. Hence, RoF systems exploiting the W-band can expand the transmission reach and capacity of wireless data service [1]. Faced with increasing demands for high-bandwidth services, higher-order modulation format, frequency division multiplexing, and constellation shaping are the enabling technologies for the next-generation optical communication [2]. In the W-band RoF system with limited receiver bandwidth, orthogonal frequency division multiplexing (OFDM) is superior to single-carrier transmission [3]. In [4], a two dual-subcarrier D-band wireless system using 64-ary quadrature amplitude modulation (QAM) can reach the data rate up to 1 Tb/s with the help of constellation shaping. In a word, OFDM with a large number of subcarriers is crucial for high spectral efficiency, while constellation shaping improves the system robustness against noises given the transmit power budget.

Probabilistic amplitude shaping (PAS) is the state-of-art coded modulation scheme. It can offer the maximum shaping gain of 1.53 dB that approaches the Shannon limit [5]. Its key elements are a systematic forward error correction (FEC) and a distribution matcher (DM) [6]. By employing a carefully designed input probability distribution according to the channel state information (CSI), it provides the system with better noise resilience and finer capacity granularity.

PAS has been investigated in single-carrier transmission [7, 8]. However, in the scenario of multi-carrier transmission such as OFDM, the PAS implementation faces a challenge of adaptivity. Since the optimal probabilistic distribution is channel-dependent, frequency selective fading (mainly caused by limited device bandwidth) leads to various subcarrier signal-to-noise ratios (SNRs). One optimal approach is bit-loading that treats each subcarrier separately [9]. It requires multiple DMs, modulation formats and an additional uplink. Alternatively, in order to implement a global probabilistic distribution, the subcarriers uniformity must be realized. This can be achieved by the precoding methods such as orthogonal circulant matrix transform (OCT) precoding [10]. Ideally, only one DM and one modulation format are required in this case, which significantly reduces the complexity. However, the concatenation of the precoding method and PAS for OFDM has seldom been studied.

In this paper, PAS combined with OCT precoding is proposed and experimentally demonstrated in a 64-QAM OFDM W-band RoF system. OCT precoding is used to equalize subcarrier noises so that all data subcarriers can be treated equally by one DM with an optimized probabilistic distribution. Moreover, when probabilistic shaping is used in the OFDM, we analyze that the bit-level achievable information rate (AIR) cannot reflect the gain brought by OCT precoding. The experimental results show that the OCT-based single-carrier PAS implementation grants the system with capacity granularity, flexibility and shaping gain.

II. Principles

A. PAS for Single-Carrier QAM Transmission

The rectangular 2^{2m}-QAM constellation can be divided into two independent 2^m-pulse amplitude modulation (PAM) constellations. We define the symbol set of each PAM constellation as $\boldsymbol{\chi} = \{\pm A_1, \cdots, \pm A_{2^{m-1}}\}$, and the amplitude probability distribution as $\mathbf{P} = \{P_{A_1}, \ldots, P_{A_{2^{m-1}}}\}$. Obviously, in the case of unshaped uniform QAM, each symbol is chosen and transmitted with equiprobability. Thus, its probability distribution is $\mathbf{P} = \{P_{A_i} = 2^{-(m-1)}\}, (i = 1, \cdots, 2^{m-1})$. Given the employed FEC with code rate R_C, the total information rate is $R_{UNI} = 2mR_C$. By contrast, with the help of DM, PAS assigns the optimized $\mathbf{P} = \{P_{A_i}\}$ to amplitudes A_i. The amount of bit information contained per amplitude in the DM's output amplitude sequence is the rate of DM, namely R_{DM}. Regarding the design of **P**, the Maxwell-Boltzmann (MB) distribution is a

This work was supported in part by National Natural Science Foundation of China (NSFC) (61775054) and Science and Technology Project of Hunan Province (2016GK2011).

The authors are with College of Computer Science and Electronic Engineering, Hunan University, Changsha, China, 410082 (*corresponding author*: *Jing He*, e-mail: jhe@hnu.edu.cn).

TABLE I
SNR GAPS TO AWGN SHANNON LIMIT AND SHAPING GAIN OF $\mathbf{P}_1, \mathbf{P}_2, \mathbf{P}_3$ SHAPED-64-QAM (BIT-LEVEL AIR)

Rate [bits/symbol]	Shannon Limit [dB]	Uniform SNR [dB]		Gap [dB]	Shaped SNR [dB]		Gap [dB]	Gain [dB]
3.0	8.4510	16-QAM	9.3129	0.8619	$\mathbf{P}_1$ Shaped 64-QAM	8.4796	0.0286	0.8333
		64-QAM	9.4345	0.9835				0.9549
3.6	10.4633	16-QAM	12.1212	1.6579	$\mathbf{P}_2$ Shaped 64-QAM	10.5186	0.0553	1.6026
		64-QAM	11.4268	0.9635				0.9082
4.0	11.7609	64-QAM	12.7070	0.9641	$\mathbf{P}_3$ Shaped 64-QAM	11.8954	0.1345	0.8296

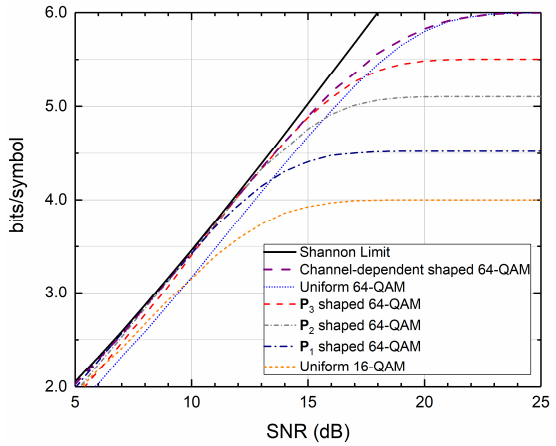

Fig. 1. Bit-level AIR of shaped and uniform QAM over AWGN channel.

common choice for the additive white Gaussian noise (AWGN) channel [5]. The total information rate of PAS-shaped QAM signal is $R_{PAS} = 2\left(R_{DM} + 1 - m(1-R_C)\right)$.

B. Bit-Level AIR

PAS adopts a FEC bit-metric decoder at the receiver. In the case of single-carrier transmission, the bit-level AIR is a good tool to predict the maximum amount of information that can be recovered by the ideal bit-metric decoding [5, 8].

For the calculation of the bit-level AIR, considering there are N samples of 1-D 2^m-PAM symbols $\mathbf{X} = \{x_1, \ldots, x_N\}$, $\left(x_j \in \boldsymbol{\chi}, j = 1, \ldots, N\right)$, according to the binary labeling rules for the modulation symbols, the corresponding sent bits are $\mathbf{B} = \{B_{1,1}, \ldots, B_{N,m}\}$. After receiving $\mathbf{Y} = \{y_1, \ldots, y_N\}$, the log-likelihood ratio (LLR) in the j-th symbol on the k-th $(k = 1, \ldots, m)$ bit level, namely $L_{j,k}$ is calculated as

$$L_{j,k} = \ln\left(\frac{\sum_{\chi \in \boldsymbol{\chi}_0^k} \exp\left(-\left|y_j - \chi\right|^2 / 2\sigma^2\right) P_X(\chi)}{\sum_{\chi \in \boldsymbol{\chi}_1^k} \exp\left(-\left|y_j - \chi\right|^2 / 2\sigma^2\right) P_X(\chi)}\right), \quad (1)$$

where $\boldsymbol{\chi}_b^i$ represents the subset of $\boldsymbol{\chi}$ containing the symbols whose i-th bit of the labeling equals b ($b = 0$ or 1), and σ^2 is the noise variance of the Gaussian auxiliary channel. $P_X(\chi)$ is the probability of the symbols, thus $P_X(\chi) = P_{A_i} / 2, (|\chi| = A_i)$. Then, the bit-level AIR can be estimated as

$$\begin{aligned} \mathrm{AIR}_{bit} \approx & \frac{1}{N}\sum_{j=1}^{N}\left[-\log_2 P_X(x_j)\right] \\ & -\frac{1}{N}\sum_{j=1}^{N}\sum_{k=1}^{m}\left[-\log_2\left(1+\exp\left((-1)^{B_{j,k}}\left(-L_{j,k}\right)\right)\right)\right]. \end{aligned} \quad (2)$$

According to (1) and (2), the bit-level AIR can be regarded as the function of the employed constellation $\boldsymbol{\chi}$, the input probability distribution $\mathbf{P}$, the channel SNR as well as the labeling rules. Since the adopted 1-D labeling rule is Gray labeling, it can be represented as

$$\mathrm{AIR}_{bit} = f(\boldsymbol{\chi}, \mathbf{P}, SNR) \quad (3)$$

TABLE II
FIXED PROBABILITY DISTRIBUTIONS OF 64-QAM ($m = 3$)

Parameters	$\mathbf{P}_1$	$\mathbf{P}_2$	$\mathbf{P}_3$
Optimized SNR [dB]	6.50	10.70	13.65
1-D Probability Distribution			
P_{A_1}	0.6254	0.5178	0.4371
P_{A_2}	0.2988	0.3241	0.3210
P_{A_3}	0.0683	0.1270	0.1732
P_{A_4}	0.0075	0.0311	0.0687
H($\mathbf{P}$) [bit]	1.2613	1.5523	1.7516

The AIR of 2-D QAM is the sum of AIRs of its divided 1-D PAMs. Fig.1 presents the bit-level AIRs for QAM vs. SNRs in different cases of $(\boldsymbol{\chi}, \mathbf{P})$. For the channel-dependent shaped 64-QAM, the input $\mathbf{P}$ is always optimized at the current operating point. Hence, it yields the performance near the Shannon limit. In addition, the MB distributions $\mathbf{P}_1/\mathbf{P}_2/\mathbf{P}_3$ are employed in the paper, which are optimized at 6.50/10.70/13.65 dB respectively. Table I displays the shaping gains of $\mathbf{P}_1/\mathbf{P}_2/\mathbf{P}_3$, and Table II summarizes their parameters. As the SNR increases, every AIR curve reaches its maximum rate, $R_{PAS}{}^* = 2\left(H(\mathbf{P})+1\right)$ or $R_{UNI}{}^* = 2m$. Furthermore, in Fig.1, the curves can be regarded as the ones of concave functions, and they are approaching the Shannon limit within their quasi-linear segment.

C. OCT Precoding for OFDM Transmission

As mentioned in the previous section, considering the practical CSI (e.g., channel SNR) is crucial for optimizing the input $\mathbf{P}$. However, in the scenario of OFDM with dozens of subcarriers, frequency selective fading effect results in hugely different SNRs among subcarriers. It is a challenge to design the probability distribution for each subcarrier separately. However, applying a fixed probabilistic distribution to a small range of SNR (around 5 dB) is a practical choice with marginal performance loss [8]. Thus, if the subcarrier SNRs concentrate within the small range, a globally designed input $\mathbf{P}$ can be applied to all subcarriers, and the single-carrier PAS implementation can extend to OFDM.

This can be done by OCT precoding [10,11]. It cannot improve the actual channel condition but spread the noises across all subcarriers. The effect of OCT precoding can be explained as follows. Given N_C data subcarriers and a $1 \times N_C$

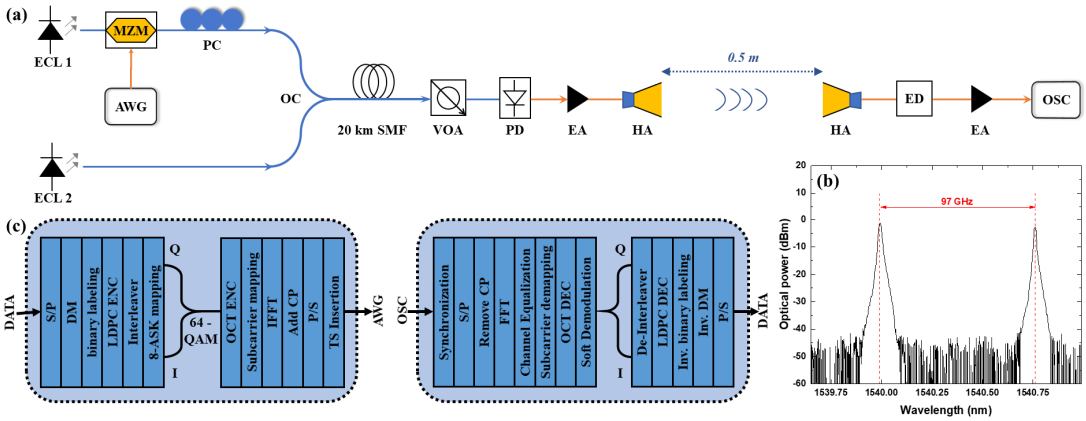

Fig. 2. (a) Experimental setup and (b) the measured optical spectrum after the OC processing. (c) Data-processing flowchart in transmitter and receiver.

vector of data subcarrier SNRs at the receiver, i.e. $\mathbf{SNR}=[SNR_1,\cdots,SNR_{N_C}]$, let $\mathbf{SNR}^{\mathrm{OCT}}$ denotes the vector with OCT, while $\mathbf{SNR}^{\mathrm{NP}}$ denotes that without any precoding method. Hence, ideally speaking,

$$\mathbb{E}[\mathbf{SNR}^{\mathrm{NP}}]=\mathbb{E}[\mathbf{SNR}^{\mathrm{OCT}}]=SNR_n^{\mathrm{OCT}},(n=1,\ldots,N_C), \quad (4)$$

where $\mathbb{E}[\cdot]$ stands for expectation.

D. Bit-level AIR for OFDM transmission

Based on our previous discussion, we then analyze that in the investigated OFDM system with N_C data subcarriers, the bit-level AIR cannot well reflect the gain brought by OCT precoding. Given the fixed $(\boldsymbol{\chi},\mathbf{P})$, (3) can be simplified as $\mathrm{AIR}_{bit}=f(SNR)$. Therefore, it can be concluded from (2) that the total bit-level AIR of the OFDM system is

$$\begin{aligned}\mathrm{AIR}_{bit} &= f(\mathbf{SNR})\\ &= f(SNR_1)+f(SNR_2)+\cdots+f(SNR_{N_C}).\end{aligned} \quad (5)$$

Fig. 1 shows that probabilistic shaping is only worthwhile to be performed for reaching the Shannon limit, where the bit-level AIR is a quasi-linear approximation to operating SNR. Therefore, according to (4), $f(\mathbf{SNR}^{\mathrm{NP}})\approx f(\mathbf{SNR}^{\mathrm{OCT}})$, i.e., their AIRs are close regardless of using OCT or not.

III. Experimental Setup and Results

Fig. 2(a) shows the experimental setup of the 64-QAM OFDM W-band RoF system. At the transmitter, two external cavity lasers (ECLs) output continuous wave (CW) lightwaves spaced by 97 GHz. The baseband signal is loaded into an arbitrary waveform generator (AWG) to drive the Mach–Zehnder modulator (MZM) via intensity modulation. After it passes through a polarization controller (PC), the CW lightwaves are combined by the optical coupler (OC) with optical spectrum in Fig. 2(b). After 20-km single-mode fiber (SMF) transmission, the total optical power is adjusted by a variable optical attenuator (VOA). The coupled lightwave is heterodyne beat in a 100-GHz photodiode (PD) to generate the 97-GHz W-band signal. It is boosted by an electrical amplifier (EA) and then beamed by a horn antenna (HA). After 0.5-m wireless transmission, the signal is received by another HA. The envelope detector (ED) implements down-conversion to yield the baseband signal. It is boosted by a 4-GHz EA and captured by an oscilloscope (OSC). Fig. 2(c) illustrates the processing of the PAS-shaped 64-QAM OFDM signal. The IFFT size is 512 and 240 subcarriers are loaded with data. The length of the cyclic prefix (CP) is 16. An optimized bit-level interleaver is adopted. After parallel-to-serial (P/S) conversion, one independent 672-point Golay-complementary training sequence (TS) is inserted for equalization and synchronization [12]. The DVB-S.2 standard low-density parity-check code (LDPC) is employed, whose decoder implements 50 iterations.

TABLE III
Key Parameters of PAS/Uniform Scheme at Different Rates

Rate [bits/symbol]	Scheme	m	R_C	R_{DM}
3.0	Uniform 16-QAM	2	3/4	—
	Uniform 64-QAM	3	1/2	—
	$\mathbf{P}_1$ Shaped 64-QAM	3	3/4	1.25
3.6	Uniform 16-QAM	2	9/10	—
	Uniform 64-QAM	3	3/5	—
	$\mathbf{P}_2$ Shaped 64-QAM	3	3/4	1.55
4.0	Uniform 64-QAM	3	2/3	—
	$\mathbf{P}_3$ Shaped 64-QAM	3	3/4	1.75

We evaluate the performance at a variety of PD input powers. Hence, by using the shaping schemes, the reduction of PD input power indicates shaping gain in terms of system sensitivity. Firstly, the bit-error rate (BER) is compared to reveal the influence of OCT precoding on PAS and uniform scheme, and at least 10^6 bits are measured for each scheme. To make a fair comparison, they achieve the same rates at 3.0/3.6/4.0 bits/symbol, with corresponding net data rates of 1.36/1.63/1.81 Gb/s. Table III gives key parameters, which shows that PAS adapts to the rates via only adjusting the DM. By comparing their BERs in Fig. 3, it shows that OCT brings more gains to PAS than uniform scheme. On the one hand, the BER improvement brought by OCT precoding for uniform 16/64-QAM decreases as the total rate increases. In Fig. 3(c), there is nearly no improvement for uniform 64-QAM with OCT precoding. Because the code rate R_C is increased in order to achieve a higher information rate, the BER performance of the employed LDPC is less sensitive to the change of SNR with higher R_C. For example, as R_C approaches 1, the LDPC's curve of BER vs. SNR tends to be flatter. Therefore, in the case of using higher R_C without OCT, even the subcarriers have quite different SNRs, their BERs are similar. On the other hand, shaping gains are observed only when OCT precoding is used. At BER of 10^{-4}, PAS can provide shaping gain of 0.91 dB compared to the uniform 16-QAM as shown in Fig. 3(a). In Fig. 3(b) and (c), compared to the uniform 64-QAM, the shaping

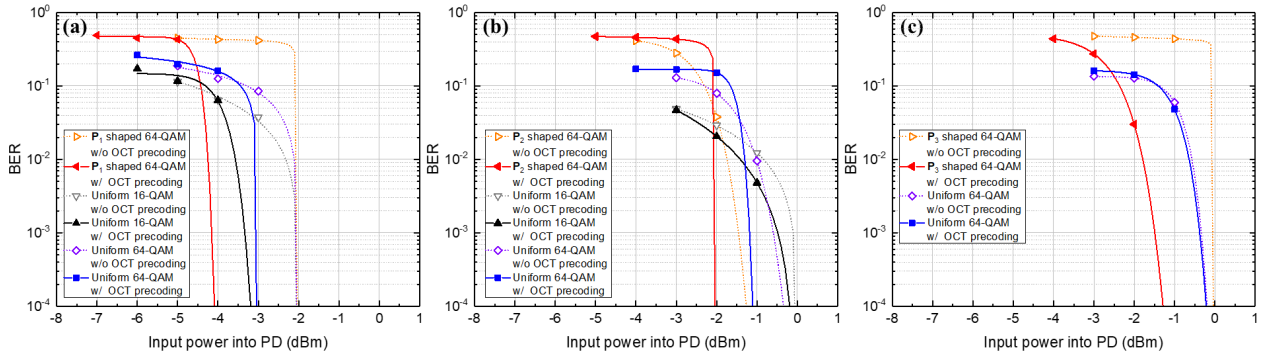

Fig. 3. BER fitting curve vs. input power into PD of shaped and uniform scheme. $R_{UNI} = R_{PAS}$ = (a) 3.0; (b) 3.6; (c) 4.0 (bits/symbol).

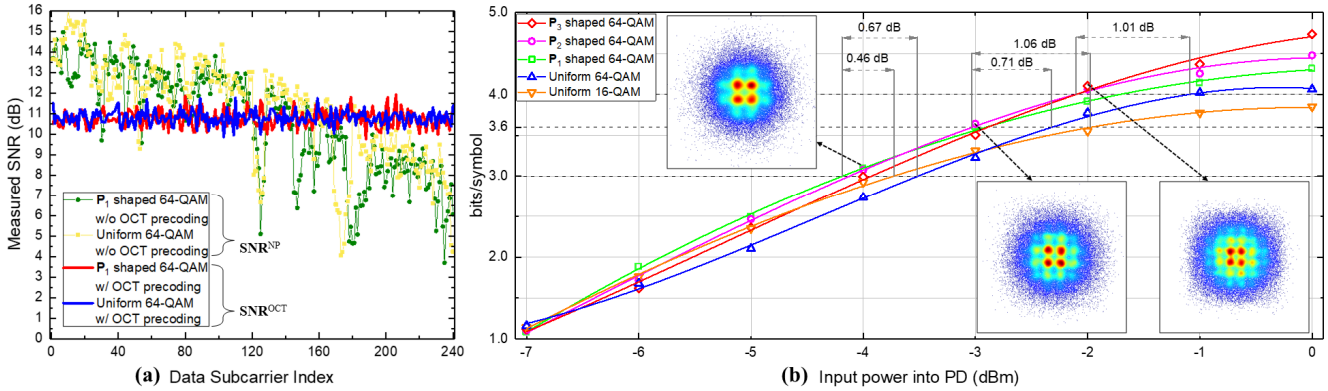

Fig. 4. (a) Measured SNR vs. data subcarrier at -3 dBm of PD input power. (b) Measured AIR vs. PD input power with OCT precoding.

gains are 0.95 and 1.07 dB respectively. The reason behind this is that the errors output by LDPC decoder are amplified by the inverse DM. Even slightly more bit errors existing in low-SNR subcarriers can have a large impact on the overall BER.

Fig. 4(a) shows $\mathbf{SNR}^{NP}$ and $\mathbf{SNR}^{OCT}$ for the $\mathbf{P}_1$ shaped and uniform 64-QAM at the input power of -3 dBm. The $\mathbf{SNR}^{NP}$ is fluctuant around 3~16 dB, while the $\mathbf{SNR}^{OCT}$ is centered around 10.74 dB within the range of 2 dB. The $\mathbf{SNR}^{NP}$ mildly exceeds the quasi-linear zone (reaching 16 dB), and the actual measured AIR of using OCT is slightly larger than that of not using OCT due to the property of the concave function.

Since OCT precoding enables the single-carrier PAS for OFDM, Fig. 4(b) illustrates the shaping gains with respect to the bit-level AIR. Three shaped signals provide shaping gains of 0.46 (compared to uniform 16-QAM), 0.71 and 1.01 dB (compared to uniform 64-QAM) at three rates respectively. Since the employed LDPC is not an ideal FEC, the rate-achieved input optical powers are smaller than that of BER results. Moreover, it's noticeable that in the case of 3 bits/symbol, system sensitivity shaping gains are not in accordance with the shaping gains in Table I. In addition, as the input power into PD increases, each curve tends to saturate at certain points. It's because there exists an optimum operating power for the PD, which means raising the input power won't improve the effective SNR linearly.

IV. Conclusion

In the paper, PAS combined with OCT precoding is proposed and experimentally demonstrated in a 64-QAM OFDM W-band RoF system with 20-km SMF and 0.5-m wireless transmission. Experimental results show that OCT precoding enables the single-carrier PAS implementation to adapt to OFDM. By merely using one DM, it provides the OFDM system with flexibility and small capacity granularity. In contrast to uniform 64-QAM, at rate of 4 bits/symbol, shaping gains are observed in terms of input power into PD, which are 1.07 dB for BER at 10^{-4}, and 1.01 dB for the bit-level AIR respectively.

References

[1] T. P *et al.*, "Photonic Millimeter-Wave System for High-Capacity Wireless Communications," *J. L. Tech.*, vol. 33, no. 1, pp. 57–67, 2015.

[2] K. Roberts, *et al.*, "Beyond 100 Gb/s: Capacity, Flexibility, and Network Optimization," *J. Opt. Commun. Netw.*, vol. 9, no. 4, p. C12, 2017.

[3] X. Li, *et al.*, "Large Capacity Optical Wireless Signal Delivery at W-Band: OFDM or Single Carrier?," *Opt. Fiber Commun. Conf.*, p. TU2B.6, 2016.

[4] X. Li, *et al.*, "1-Tb/s Photonics-aided Vector Millimeter-Wave Signal Wireless Delivery at D-Band," *Opt. Fiber Commun*, Th4D.1, 2018.

[5] G. Böcherer, P. Schulte, and F. Steiner, "Bandwidth Efficient and Rate-Compatible Low-Density Parity-Check Coded Modulation," *IEEE Trans. Commun.*, vol. 63, no. 12, pp. 1–14, 2015.

[6] P. Schulte and G. Böcherer, "Constant composition distribution matching," *IEEE Trans. Inf. Theory*, vol. 62, no. 1, pp. 430–434, 2016.

[7] F. Buchali, G. Bocherer, *et al.*, "Experimental demonstration of capacity increase and rate-adaptation by probabilistically shaped 64-QAM," *Eur. Conf. Opt. Commun. ECOC*, vol. 2015–Novem, no. 2, pp. 2–4, 2015.

[8] T. Fehenberger, A. Alvarado, G. Bocherer, *et al.*, "On Probabilistic Shaping of Quadrature Amplitude Modulation for the Nonlinear Fiber Channel," *J. Light. Technol.*, vol. 34, no. 21, pp. 5063–5073, 2016.

[9] F. Steiner *et al.*, "Approaching Waterfilling Capacity of Parallel Channels by Higher Order Modulation and Probabilistic Amplitude Shaping," *2018 52nd CISS*, Princeton, NJ, 2018, pp. 1-6.

[10] Y. Hong, X. Guan, L. Chen, and J. Zhao, "Experimental Demonstration of an OCT-based Precoding Scheme for Visible Light Communications," *Opt. Fiber Commun. Conf. 2016*, pp. 3–5, 2016.

[11] Y. Wei, *et al.*, "An approach enabling adaptive FEC for OFDM in fiber-VLLC system," *Opt. Commun.*, vol. 405, no. Sep, pp. 329–333, 2017.

[12] J. He, C. Xiang, F. Long, K. Wu, and L. Chen, "Pre-compensation combined with TS-aided and ISFA-enhanced scheme for UWB system," *Opt. Commun.*, vol. 396, no. March, pp. 150–155, 2017.